Recent Progress of Organometal Halide Perovskite Solar Cells

JOTARO NAKAZAKI[1], HIROSHI SEGAWA[1,2]
[1] RESEARCH CENTER FOR ADVANCED SCIENCE AND TECHNOLOGY,
THE UNIVERSITY OF TOKYO, 4-6-1 KOMABA, MEGURO-KU, TOKYO 153-8904, JAPAN
[2] DEPARTMENT OF GENERAL SYSTEMS STUDIES,
GRADUATE SCHOOL OF ARTS AND SCIENCES,
THE UNIVERSITY OF TOKYO, KOMABA 3-8-1, MEGURO-KU, TOKYO 153-8902, JAPAN.

ABSTRACT

Organometal halide perovskites solar cells have gathered wide interest from various research fields. A power conversion efficiency of over 22% was achieved within a few years from their advent. In this review article, publications about perovskite solar cells are summarized in order of their submission dates to show the trends in the development of various types of devices. At the first stage, perovskite solar cells were established as nanostructured solar cells. Efficiencies of up to 15% attracted researchers in dye-sensitized solar cells and organic thin-film solar cells. Since the appearance of planar hetero-junction type solar cells, the power generation mechanism of perovskite solar cells has been argued. At present, the highest efficiency in published papers is 21.8%, and the efficiency table records 22.1%. A summary of the development history of perovskite solar cells in early days is presented.

KEYWORD

Organometal halide, Perovskite, Solar cell, Printable device

INTRODUCTION

The development of low-cost solar cells has been a worldwide important subject. Solar cells based on organometal halide perovskites have captured current interest as a promising candidate for low-cost high-efficiency solar cells. These devices were classified as perovskite solar cells in any research field, including "Solar cell efficiency tables" of the journal Prog. Photovolt. Res. Appl. [1] or "Best Research-Cell Efficiencies" chart by NREL [2].

Most of the materials for perovskite solar cells can be supplied at low cost. Although some materials are expensive at present, they can be replaced by another material or the cost can be reduced by mass production. Due to the solution printable process, vacuum chambers or high-temperature processes are not needed. Therefore, the costs for facilities or energy consumption can be reduced. Revolutionally low production costs are expected for perovskite solar cells. The highest power conversion efficiency of perovskite solar cells in the NREL chart (Rev. 04-14-2017) is 22.1%, which is comparable to those of polycrystalline Si solar cells (21.9%), CIGS solar cells (22.6%), and CdTe solar cells (22.1%). Such a high efficiency can be accomplished with low cost.

Publications on perovskite solar cells are increasing rapidly. Nowadays, "publication year" alone is no longer adequate for describing when the results were reported. Fig.1 shows the statistics for publications about perovskite solar cells counted by their submission or publication (online) months. The number of publications is growing month by month. Even within a year, for example, March and August might be classified into different development stages. In some cases, the background of research upon submission was completely changed when the paper was published.

In this review article, publications about perovskite solar cells were comprehensively summarized in terms of their "submitted date", to show the trends in the development of various types of devices. In particular, the reports from the early days are fully described. The following sections represent each stage of the progress in this field.
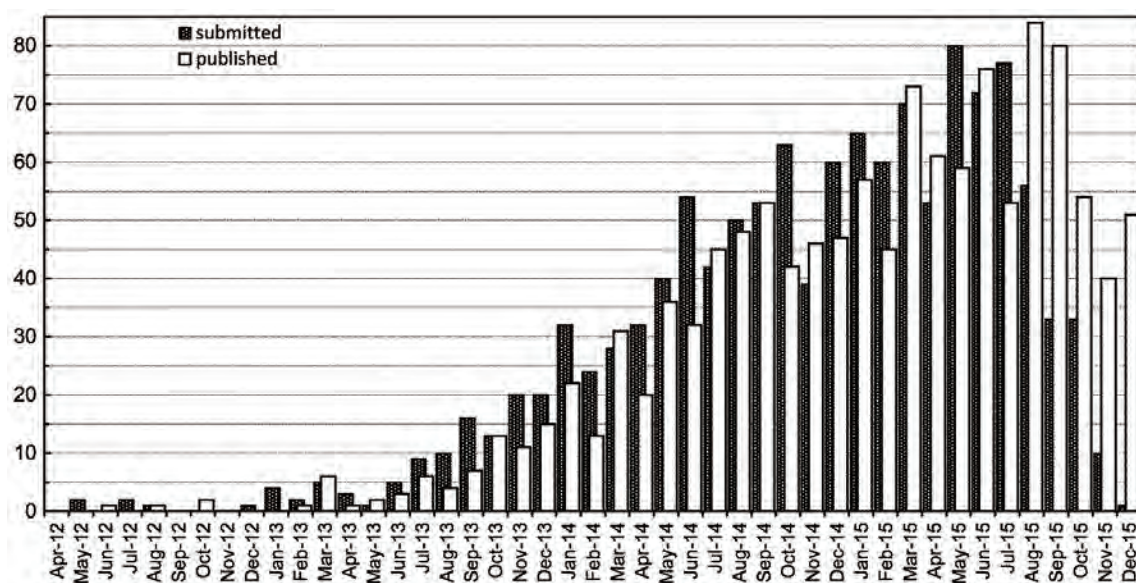
Fig. 1: Statistics for publications about perovskite solar cells counted by their submission or publication months.

ADVENT OF MESOSCOPIC PEROVSKITE SOLAR CELLS

Perovskite solar cells have originated from the studies on dye-sensitized solar cells (DSCs). In the course of the development of dye-sensitized solar cells, various sensitizing dyes have been reported [3]. Quantum dot sensitized solar cells have been also developed to replace the organic-based dyes with inorganic materials [4]. Under such circumstances, the organometal halide perovskites were used as sensitizers in photoelectrochemical cells [5]. They used nano-particular $CH_3NH_3PbBr_3$ or $CH_3NH_3PbI_3$ instead of dyes. The power generation in DSCs is based on electron injection from photo-excited dye to TiO_2 followed by regeneration (reduction) of the oxidized dye with iodide anion. Perovskite-sensitized solar cells were explained by a mechanism similar to that of DSCs. For the preparation of perovskite-sensitized solar cells, the precursor solution was spin-coated over a mesoporous TiO_2 film on a FTO glass substrate, and the resulting photo-anode was assembled with a counter electrode of Pt-coated FTO glass and the insertion of a 50 μm thick separator film. The gap between the electrodes was filled with an electrolyte solution containing lithium halide and halogen as a redox couple. Different from quantum dot sensitized solar cells, in which quantum dots were prepared in advance, the perovskite sensitizer was directly prepared on the substrate. Although those perovskite-sensitized cells exhibited a power conversion efficiency of 3.81%, they had a problem with durabil-

ity. The potential of perovskite-sensitized solar cells was emphasized in a Perspective Article [6]. Following their work, Park et al. improved the preparation condition to obtain 6.5% efficiency in the solar cells [7]. In addition to $CH_3NH_3PbI_3$, $CH_3CH_2NH_3PbI_3$ was also examined [8]. Miyasaka et al. found that $CH_3NH_3PbBr_3$ exhibits strong emission on Al_2O_3 or ZrO_2 [9], while its emission was not detectable on TiO_2 or SnO_2, indicating efficient electron injection in the latter cases.

Since the liquid electrolytes seemed to be a cause of the durability problem, some groups independently tried to prepare all-solid perovskite sensitized solar cells. On May 2012, Snaith et al. submitted a paper on solar cells based on meso-superstructured organometal halide perovskites [10]. They used 2,2',7,7'-tetrakis-(N,N-di-p-methoxyphenylamine)-9,9'-spirobifluorene (spiro-OMeTAD) as a hole conductor, instead of an iodine/iodide-based liquid electrolyte. As the precursor solution for perovskite formation, they used a N,N-dimethylformamide (DMF) solution of $PbCl_2$ and CH_3NH_3I. Therefore, the perovskites were denoted as $CH_3NH_3PbI_2Cl$. A device using mesoporous TiO_2 exhibited a power conversion efficiency of 7.6%, while a device using Al_2O_3 showed 10.9% efficiency. Another device using Al_2O_3 showed a high Voc of 1.13 V. In the case of Al_2O_3-based devices, the electron injection from perovskite to the conduction band of Al_2O_3 is not possible. Therefore, they explained that the electrons pass through the thin perovskite layer (perovskite skin) to the

FTO electrode. Such a system was termed as meso-super-structured solar cell. This paper was published online on Oct. 4, 2012. On July 2012, Park et al. submitted a paper on perovskite sensitized all-solid-state mesoscopic solar cells [11]. This paper was published online on Aug. 21, 2012, to be the first report on all-solid perovskite solar cells, earlier than the paper of Snaith et al. Park et al. assumed a power generation mechanism similar to that in dye-sensitized solar cells. They reported a power conversion efficiency of 9.7%. In this paper, the electron injection from perovskite to the conduction band of TiO_2 was observed after the hole injection from perovskite to the spiro-MeOTAD hole conductor. These two papers became the sources of two major streams in the studies on perovskite solar cells: the former one includes chloride-containing perovskites ($CH_3NH_3PbI_{3-x}Cl_x$) and doesn't rely on the sensitization mechanism, while the latter one is composed of all iodide perovskites ($CH_3NH_3PbI_3$) and is based on the sensitization mechanism.

In addition to these two papers, two more papers were submitted before the publication of the report of meso-superstructured cells. On July 2012, Seok et al. submitted a paper on perovskite solar cells using polymeric hole conductors [12]. They reported a power conversion efficiency of 12.0%, which was comparable to the highest efficiency in dye-sensitized solar cells at that time (12.1% [13]). If the paper had appeared immediately, it might have had a great impact. However, it was published on May 5, 2013, and was almost dismissed because of the impact of another report of 15% efficiency at a conference. The other paper was submitted on August 2012 by Etgar et al. [14]. A power conversion efficiency of 5.5% was reported without using a hole transport layer.

Following these first reports, several papers were submitted in early 2013. As seen in the above cases, the order of publication sometimes doesn't reflect the order of the invention. Therefore, the reports will be arranged according to the submitted date of the papers in the following sections. Snaith et al. (Dec. 11, 2012) prepared mesoporous particles composed of TiO_2 single crystals by crystal growth on mesoporous SiO_2 particle followed by a silica-etch process [15]. Using these TiO_2 particles, a perovskite solar cell with 7.3% efficiency was prepared without a sintering process. S. Yang et al. (Jan. 12, 2013) applied $CH_3NH_3PbI_3$ and $CH_3NH_3PbI_2Br$ to TiO_2 nanowire arrays to afford a power conversion efficiency of 4.87% for $CH_3NH_3PbI_2Br$ [16]. Park et al. (Jan. 23, 2013) used TiO_2 rutile nanorods sensitized

with $CH_3NH_3PbI_3$ to get 9.4% efficiency [17]. Seok et al. (Jan. 28, 2013) tuned the ratio of Br and I in $CH_3NH_3Pb(I_{1-x}Br_x)_3$ perovskites to control their band gap, enabling the achievement of colorful solar cells [18]. In the best case, a power conversion efficiency of 12.3% was obtained. As seen here, high efficiencies were reported by balancing the wide absorption band of iodide-based perovskites and the high voltage derived from bromide-based perovskites. Zhang, Qiu, et al. (Jan. 30, 2013) applied a polymeric hole conducting material for $CH_3NH_3PbBr_3$ and $CH_3NH_3PbI_3$-based solar cells [19]. Hodes et al. (Feb. 15, 2013) applied a perylenediimide derivative as the hole conductor in $CH_3NH_3PbBr_3$-based solar cells to achieve a high Voc of 1.3 V [20]. Snaith et al. (Mar. 8, 2013) reported a meso-superstructured perovskite solar cell with 12.3% efficiency [21]. In this case, the perovskite formed a layer with ca. 300 nm thickness, indicating that the sensitization mechanism is not needed for efficient power generation. The mesoporous Al_2O_3 layer was regarded just as a scaffold for the perovskite layer. Snaith et al. (Mar. 21, 2013) put a fullerene monolayer between TiO_2 and perovskite [22]. Compared to the sample without the fullerene layer (10.2%), an improved efficiency of 11.7% was obtained. This was explained as being due to the fullerene layer inhibiting electron injection to TiO_2, where the electron transport is slow. Charge transport in the perovskite layer was found to be very fast leading to higher efficiency. Johansson et al. (Mar. 22, 2013) compared three hole conductors, and showed that spiro-OMeTAD was the best because of its long electron diffusion lifetime [23]. 8.5% efficiency was obtained. P. Chen et al. (Mar. 25, 2013) reported an inverted structure perovskite solar cell for the first time [24]. All the previous cells transported electrons toward TCO side. In the case of the inverted structure, a hole conductor (PEDOT:PSS) layer is prepared at the TCO side, then an electron acceptor (C60 etc.) layer is put over the perovskite layer. The structure is similar to that of organic thin-film solar cells. The best cell by Chen et al. showed 3.9% efficiency. Hagfeldt et al. (Mar. 28, 2013) applied $CH_3NH_3PbI_3$ to ZnO nanorod arrays to achieve 5.0% efficiency [25].

On Apr. 3, 2013, Grätzel et al. submitted a paper reporting 15% efficiency [26]. They prepared a perovskite layer by "sequential deposition". The method itself had been reported 15 years earlier by Mitzi et al. [27]. At first, a PbI_2 layer was deposited, and then, it was converted to perovskite by immersing it in a CH_3NH_3I solution. The difference is that the perovskite layer was prepared on
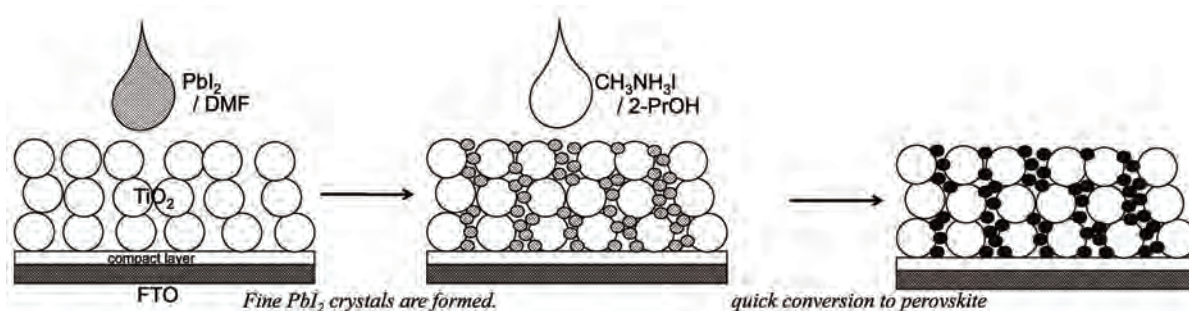
Fig. 2: Schematic drawings for perovskite preparation with sequential deposition method.

nanoporous TiO_2 in this case. Since the conversion from PbI_2 to $CH_3NH_3PbI_3$ is achieved by the permeation of CH_3NH_3I into PbI_2 crystals, the existence of large PbI_2 crystals makes it difficult. The formation of PbI_2 crystals in nanoporous TiO_2 regulates the size of PbI_2 crystals, leading to a quick reaction with CH_3NH_3I (Fig.2). High-quality perovskites were formed by such technique.

Consideration of perovskites on the basis of band structure, which was derived from crystallographic analyses, was suggested by Baikie et al. [28]. Although the crystal structures of perovskites had been already known by the report of Poglitsch et al. in 1987 [29], they performed more precise analyses, such as the temperature dependence of lattice parameters.

RISE OF PLANAR HETERO-JUNCTION PEROVSKITE SOLAR CELLS

The paper reporting 15% efficiency was published on Jul. 10, 2013. Therefore, the papers submitted prior to July could be considered as independent achievements. The papers submitted before early September are reviewed here in order of submission date. In this period, the role of mesoporous oxide layer was reconsidered. Worsley et al. (Jun. 3, 2013) reported a one-step low temperature processing route, where Al_2O_3 nanoparticles were mixed with the perovskite precursor, without preparing a mesoporous layer in advance [30]. 7.2% efficiency was reported. L. Wang et al. (Jun. 10, 2013) prepared perovskite-sensitized solar cells with liquid electrolyte [31]. By covering the perovskite surface with thin layer of Al_2O_3, both the dissolution of perovskite into the electrolyte solution and charge recombination between electrons in the TiO_2 conduction band and holes in the electrolyte were reduced to achieve 6.0% efficiency.

On Jun. 19, 2013, Snaith et al. submitted two papers about planar hetero-junction perovskite solar cells, which were prepared by a vapour deposition process [32] or a solution process [33]. In the latter paper, they applied the procedures used in meso-superstrucutured perovskite solar cells to the substrates without a mesoporous layer, and achieved 11.4% efficiency by controlling the perovskite morphology through the modification of preparation conditions. In the former paper [32], they prepared a perovskite layer by dual-source vapour deposition process, which was reported by Era et al. in 1997 [34]. Snaith et al. succeeded in preparing a $CH_3NH_3PbI_{3-x}Cl_x$ layer on a TiO_2 compact layer to achieve 15.4% efficiency, the highest value at that time. Through these studies, a mesoporous oxide layer proved to be not necessary.

Hagfeldt et al. (Jun. 26, 2013) applied the two-step deposition technique to prepare $CH_3NH_3PbI_3$ perovskites on mesoporous TiO_2 and ZrO_2, achieving 9.5% and 10.8% efficiencies, respectively [35]. Snaith et al. (Jul. 2, 2013) incorporated gold nanoparticles with a SiO_2 shell into the perovskite/Al_2O_3 mesoporous layer to achieve 11.4% efficiency [36]. Snaith et al. (Jul. 6, 2013) reported that Al_2O_3-based perovskite solar cells have an advantage in stability with respect to UV light compared to TiO_2-based cells [37]. Etgar et al. (Jul. 7, 2013) improved the efficiency of hole conductor-free perovskite solar cells up to 8.04% [38], where the thickness of the perovskite layer was increased from the former report [14]. Zhu et al. (Jul. 18, 2013) investigated charge transport and recombination processes in perovskite-sensitized liquid electrolyte-based solar cells [39]. L. T. Yan et al. (Aug. 8, 2013) tried to reproduce solar cells based on $CH_3NH_3PbI_xCl_{3-x}$, but the resulting efficiency was only 0.28% [40]. Hanaya et al. (Aug. 20, 2013) reported co-sensitization of TiO_2 by dyes and perovskites [41].

Manufactured modules are necessary for the practical use of solar cells. Di Carlo et al. (Aug. 9, 2013) reported solid-state solar modules based on mesoscopic $CH_3NH_3PbI_{3-x}Cl_x$ perovskite for the first time [42]. They prepared a monolithic module composed of 5 series-connected cells with dimensions of 48 mm × 7 mm (total active area: 16.8 cm^2). Using P3HT as a hole conductor, Voc of 4.45 V, Isc of 36.8 mA, FF of 52.6%, and PCE of 5.10% were obtained. H. Han et al. (Aug. 25, 2013) prepared monolithic hole-conductor-free perovskite solar cells [43]. A mesoporous TiO_2 layer, ZrO_2 layer, and carbon layer were stacked, then perovskite precursor solution was penetrated from the carbon side. 6.53% efficiency was obtained. In this case, carbon itself works as a counter electrode, and metal deposition is not needed. They (Sep. 10, 2013) improved the carbon material to obtain 6.64% efficiency [44]. Since there is no vacuum deposition process, they claimed this device to be a fully printable solar cell.

Mathews et al. (Aug. 27, 2013) reported low-temperature processed ZnO-based flexible perovskite solar cells [45]. Until this time, a TiO_2 compact layer had been necessary for perovskite solar cells, except for one case (inverted structure [24]). Preparation of TiO_2 compact layers requires sintering processes, and is not compatible for plastic substrates. A ZnO compact layer was prepared by cathodic electrodeposition. FTO-glass substrate devices and ITO-PET substrate devices were fabricated achieving 8.90% and 2.62% efficiency, respectively. L. Wang et al. (Sep. 9, 2013) reported the post-modification of perovskite layers [46] to cover them with a thin Al_2O_3 layer, which was previously reported for liquid electrolyte cells [31]. The efficiency of the all-solid cell without post-modification decreased from 4.69% to 0.942% after 18 h, while that of the cell with post-modification decreased from 4.60% to 2.23%, maintaining 48% of its initial value. Di Carlo et al. (Sep. 10, 2013) improved the efficiency of the cells using P3HT as a hole conductor to 9.3% [47]. Boix et al. (Sep. 11, 2013) used electrospun TiO_2 nanofibers as a mesoporous layer to achieve 9.8% efficiency [48]. Bolink et al. (Sep. 16, 2013) reported the 2nd example of inverted structure perovskite solar cells [49]. A poly-triarylamine derivative (poly-TPD) layer was inserted between the PEDOT:PSS layer and the $CH_3NH_3PbI_3$ layer. The perovskite layer was prepared by vacuum deposition. All layers were prepared by spin-coating or vacuum deposition to achieve an efficiency of 12.04%. These processes are compatible with flexible substrates. Kelly et al. (Sep. 16, 2013) used ZnO nanoparticle layers as the oxide part of perovskite solar cells without a sintering process [50]. The planar hetero-junction perovskite solar cell exhibited a power conversion efficiency of 15.7%, which was the highest value at that time. They also prepared a flexible device with an ITO/PET substrate, exhibiting an efficiency of 10.2%.

Studies of the power generation mechanism or the physical properties of the materials were also performed at this time. Bisquert et al. (Apr. 10, 2013) described the mechanism of carrier accumulation in perovskite solar cells [51]. Sum et al. (Jul. 12, 2013) and Snaith et al. (Jul. 30, 2013) independently described carrier transport in the perovskite layer, by observing the quenching of photoluminescence [52, 53]. Sum et al. described long-range balanced transport of electrons and holes in $CH_3NH_3PbI_3$ [52]. Snaith et al. showed electron-hole diffusion lengths in $CH_3NH_3PbI_{3-x}Cl_x$, which exceeded 1 micrometer, longer than those in $CH_3NH_3PbI_3$ [53]. Such carrier transport is a reason for high efficiency in perovskite solar cells. Moser et al. (Jul. 13, 2013) explained that primary charge separation occurs at both junctions, with TiO_2 and the hole-transporting material, simultaneously, with ultrafast electron and hole injection taking place from the photo-excited perovskite over similar timescales [54]. Grätzel et al. (Aug. 19) reported the results of impedance spectroscopic analysis [55]. Moser et al. (Aug. 25, 2013) reported similar analysis using transient absorption spectroscopy [56]. Listorti, De Angelis, Mosca, et al. (Aug. 30, 2013) investigated the role of chloride in $CH_3NH_3PbI_{3-x}Cl_x$ perovskites [57]. Although they found some features, such as low concentration of Cl in perovskite independent to the precursor solution, the main reason for better performance of $CH_3NH_3PbI_{3-x}Cl_x$ than $CH_3NH_3PbI_3$ could not be explained clearly.

Theoretical calculations on organometal halide perovskites were also performed at this time. The first contribution was made by De Angelis et al. (May 17, 2013) [58]. The importance of spin-orbit coupling was pointed out by Even et al. (Jul. 19, 2013) [59]. Walsh et al. (Aug. 14, 2013) suggested the effect of the dipole of methylammonium cations [60]. Listorti, De Angelis, Mosca, et al. (Aug. 30, 2013) presented also calculation results [57]. Filippetti and Mattoni (Sep. 2, 2013) compared the results for $CH_3NH_3PbI_3$ and $CH_3NH_3PbI_2Cl$ [61]. Pedesseau et al. (Sep. 13, 2013) made calculations both for 2D and 3D perovskites [62].

Rapid growth in studies of perovskite solar cells was reported in an Editorial in J. Phys. Chem Lett. (published on Aug. 1, 2013) [63] and in News & Views in Nature (published on Sep. 11, 2013) [64]. Submission of review articles started at this time. Park (Apr. 27, 2013) described a plan toward 20% efficiency in a Perspective Article [65]. Diau et al. (Jul. 10, 2013) explained the status [66]. Park et al. (Sep. 9, 2013) summarized the early stage of perovskite solar cell studies in a Feature Article [67]. Snaith (Sep. 18, 2013) summarized the historic evolution from dye-sensitized solar cell and the future direction for perovskite solar cells in a Perspective Article [68]. At this point, 20% efficiency was a target for the near future, but was still far away.

A paper reporting planar hetero-junction perovskite solar cells prepared by dual-source vapour deposition process [32] was published on Sep. 11, 2013, and the planar structure received much interests.

SOLVENT ENGINEERING AND COMPOSITIONAL MODIFICATION

By September 2013, three types of perovskite solar cells, namely, mesoscopic type, planar hetero-junction type, and inverted type, had been reported as described above. The representative structures are shown in Fig.3. To clarify the improvements in each structure, Fig.4 shows the highest power conversion efficiency in each paper, plotted versus the submitted date of each paper. Among mesoscopic cells, TiO_2, ZnO, and SnO_2-based cells (filled circles) are considered as sensitized type cells, while Al_2O_3, ZrO_2, and SiO_2-based cells (open circles) are considered as meso-superstructured type cells. To simplify the description, the highest value in the paper is shown routinely without considering the main target in the paper. If the reference cell is more efficient than the target device, the efficiency of the reference cell is shown.

There were several improvements in device preparation methods. Y. Yang et al. (Nov. 12, 2013) reported a "vapor assisted solution process" for planar hetero-junction perovskite solar cells [69]. In this case, the prepared PbI_2 film was annealed at 150 °C in the presence of CH_3NH_3I to obtain perovskite film, resulting in a 12.1% efficiency. Snaith et al. (Nov. 12, 2013) prepared a TiO_2 compact layer at less than 150 °C without sintering process, to fabricate meso-superstructured perovskite solar cells [70], and achieved 15.9% efficiency. Park et al. (Feb. 7, 2014) prepared the perovskite layer by two-step spin-coating, PbI_2 followed by CH_3NH_3I [71]. By varying the concentration of the CH_3NH_3I solution, various sizes of $CH_3NH_3PbI_3$ cuboids were prepared. The highest efficiency, of up to 17.01%, was obtained in the case of low concentration CH_3NH_3I, which gave the biggest cuboids. Seok et al. (Feb. 24, 2014) investigated various solvents for spin-coating of perovskites and found the possibility of using dimethylsulfoxide (DMSO) and toluene [72]. By dripping toluene during the spin-coating procedure, they obtained 16.5% efficiency and a certified efficiency of 16.2%, which was plotted in the NREL chart. Y. Yang et al. (Mar. 28, 2014) reported 19.3% efficiency for a planar hetero-junction perovskite solar cell [73]. They featured interface engineering. Three points were raised by the authors. Firstly, they used ITO instead of FTO. To reduce the work function of ITO from 4.6 eV to 4.0 eV, the surface was modified with polyethyleneimine ethoxylate (PEIE). Secondly, they used yttrium-doped TiO_2 for the electron transport layer. Thirdly, they annealed the $CH_3NH_3PbI_{3-x}Cl_x$ perovskite layer under controlled humidity (30%RH). The third feature was very interesting, because organolead halide perovskites are usually unstable to humidity. In fact, their device performance immediately dropped under ambient condition. Controlled treatment may be important. Y.-B. Cheng et al. (May 16, 2014) used a "fast deposition-crystallization" procedure to prepare highly crystalline perovskite layers [74]. By the addition of chlorobenzene during the spin-coating of the dimethylformamide solution of perovskite precursors, densely packed crystalline perovskite layers were obtained to achieve 16.2% efficiency. As seen here, both in mesoscopic type and planar hetero-junction type cells, dripping less soluble solvent gave good results. This method has been denoted as "anti-solvent method" in recent cases.
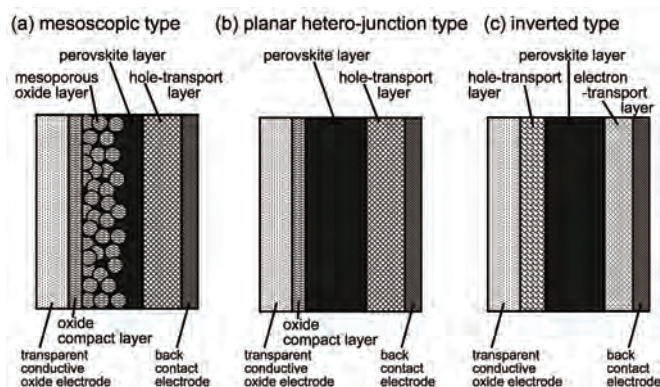

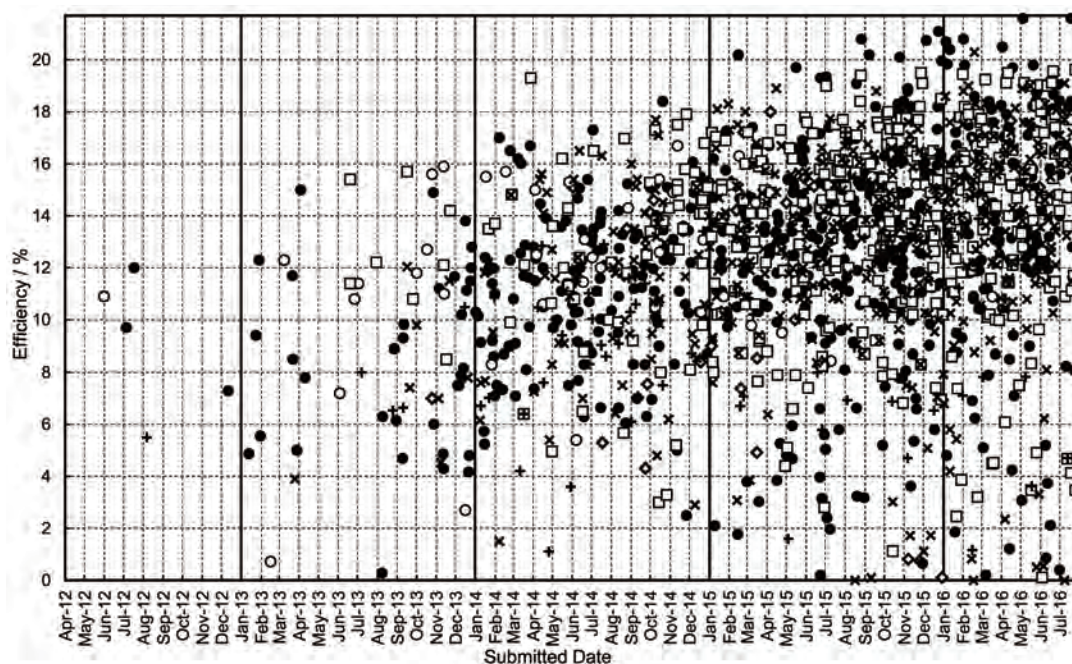**Fig. 3:** Structures of perovskite solar cells.

Fig. 4: Reported power conversion efficiencies of perovskite solar cells plotted versus the submitted date of the paper. The type of markers indicates the structure of the cell. filled circles: mesoscopic type (TiO_2, ZnO, SnO_2-based); open circles: mesoscopic type (Al_2O_3, ZrO_2, SiO_2-based); squares: planar hetero-junction type; cross: inverted type; plus: HTM-free type; diamonds: others.

Concerning the composition of perovskite materials, there are limited choices. For the metal ion, Pb and Sn are realistic choices. For the halogen, I, Br, and Cl are possible. For the counter cation, Cs, CH_3NH_3, $CH_3CH_2NH_3$, NH_2CHNH_2 are possible. Therefore, the targets of investigation have been their composition and some additives.

The first report on Sn-based perovskite solar cells was submitted by Kanatzidis et al. on Jan. 14, 2014 [75], although it appeared on May 4, 2014, later than the publication of the report by Hayase et al. on Mar. 3, 2014, which was submitted on Jan. 29, 2014 [76]. Sn-based perovskites have a lower bandgap than Pb-based perovskites. Therefore, Sn-based perovskites absorb near-IR photons. However, the bandgap is too low to generate photovoltage. In fact, in a previous study, Kanatzidis et al. (Feb. 6, 2012) used $CsSnI_{2.95}F_{0.05}$ as the hole transport material of an all-solid-state DSC [77]. In the present case, Kanatzidis et al. [75] utilized mixed halogen ($CH_3NH_3SnI_{3-x}Br_x$) to tune the bandgap, while Hayase et al. [76] utilized mixed metal ($CH_3NH_3Sn_xPb_{1-x}I_3$). Kanatzidis et al. reported 5.73% efficiency as the highest case, and an IPCE up to 950 nm, using spiro-OMeTAD as a hole transport material. Hayase et al. used P3HT as a hole transport material to show an IPCE up to 1060 nm and 4.18% efficiency. Kanatzidis et al. (Apr. 2, 2014) analyzed the fact that mixed metal perovskites ($CH_3NH_3Sn_xPb_{1-x}I_3$) show absorption at longer wavelengths than the parent materials ($CH_3NH_3PbI_3$ and $CH_3NH_3SnI_3$) [78]. Snaith et al. (Apr. 4, 2014) reported 6.4% efficiency for perovskite solar cell using $CH_3NH_3SnI_3$ [79]. Mathews et al. (May 2, 2014) used $CsSnI_3$ doped with SnF_2 to exhibit an IPCE up to 1000 nm [80]. In some cases, the "lead-free" feature of Sn-based perovskites was emphasized. Although the broad absorption of Sn-based perovskites is attractive, some breakthroughs are still needed to get better performance.

Br-based perovskites exhibit a larger bandgap than I-based perovskites. Although the photo-absorption region of Br-based perovskites is limited to shorter wavelengths, higher photovoltage is available. Cahen et al. (Dec. 16, 2013) reported perovskite solar cells with Voc ~ 1.5 V by the use of chloride-containing perovskite $CH_3NH_3PbBr_{3-x}Cl_x$ [81]. Bandgap tuning based on a mixed I-Br system had been already reported by Seok et al. [18]. Mhaisalkar et al. (Jan. 23, 2014) applied a sequential deposition method to a $CH_3NH_3PbI_{3-x}Br_x$ system [82]. Zhao and Zhu (Jul. 15, 2014) prepared $CH_3NH_3PbI_2Br$ nanosheets from PbI_2, CH_3NH_3Br, and CH_3NH_3Cl [83]. Due to CH_3NH_3Cl, a uniform and compact perovskite layer was obtained.

Replacement of the methylammonium ion (MA: $CH_3NH_3^+$) by a formamidinium ion (FA: $NH_2CHNH_2^+$) moves the photo-absorption onset of perovskites to longer wavelengths. Therefore, an increase in photocurrent is expected. The first paper reporting formamidinium-containing perovskite solar cells were submitted by Grätzel et al. on Oct. 27, 2013, although it was published as the 4th paper on Feb. 19, 2014 [84]. The papers by Baikie et al. (Nov. 12, 2013) [85], Snaith et al. (Nov. 22, 2013) [86], and Cui et al. (Dec. 6, 2013) [87] were published earlier. Grätzel et al. investigated a mixed cation system, with $MA_{0.6}FA_{0.4}PbI_3$ and achieved 14.9% efficiency [84]. Baikie et al. reported 4.3% efficiency by the use of $FAPbI_3$, the first such publication [85]. Snaith et al. used a mixed halogen system $FAPbI_{3-x}Br_x$ and obtained 14.2% efficiency [86]. Cui et al. reported 7.5% efficiency for $FAPbI_3$ by the use of P3HT as the hole transport material [87]. Among these cases, Grätzel et al., Baikie et al., and Cui et al. prepared the perovskite by a two-step method, i.e., PbI_2 was spin-coated first and then dipped into the solution of FAI or mixed FAI-MAI. Snaith et al. prepared precursor solutions of $FAPbI_3$ which contain additional HI. For $FAPbI_{3-x}Br_x$, HI and HBr were added to the precursor solution. The perovskite layer was prepared by one-step spin-coating [86]. Park et al. (Mar. 13, 2014) improved the synthetic procedure for FAI, the thickness of the porous TiO_2 layer, and the annealing temperature to obtain a good formamidinium-based perovskite layer by a two-step method [88]. By adding a thin $MAPbI_3$ layer on the $FAPbI_3$ layer, 16.01% efficiency was obtained. Cui et al. (May 15, 2014) also reported a one-step preparation of formamidinium-based perovskite containing chloride, $FAPbI_{3-x}Cl_x$, with a P3HT hole transport layer [89]. Docampo et al. (Jun. 17, 2014) reported 6.5% efficiency using $FAPbBr_3$ [90].

By Aug. 20, 2014, eleven papers reporting efficiencies higher than 16% had been submitted. Three of these reported planar hetero-junction type cells [73, 74, 91] and two papers reported inverted structure cells [92, 93]. Planar and inverted structures were regarded novel at that time, while mesoscopic devices exhibited some novel features. Therefore, novel hole transport materials [94, 95], modification of perovskite composition using Br or FA, [72, 88], or characteristic cuboid structure [71] were featured. The other standard structure cell with 17.3% efficiency was used for water photolysis [96]. In the case of meso-superstructured cells based on mesoporous Al_2O_3, four papers [70, 97, 98, 99] reported efficiencies higher than 15.5%, but less than 16%.

DEVICE OPTIMIZATION TOWARDS EFFICIENCIES ABOVE 20%

On Oct. 20, 2014, Seok et al. submitted a paper reporting 18.4% efficiency, together with certified data of 17.9% efficiency [100]. The key point was "compositional engineering" by adjusting the ratio of formamidinium lead iodide ($FAPbI_3$) and methylammonium lead bromide ($MAPbBr_3$). Although the broader photo-absorption of FA ($NH_2CHNH_2^+$) based perovskites compared with MA ($CH_3NH_3^+$) based perovskites is attractive in order to increase photocurrent [84-90], preparation of pure perovskites using FA was difficult. In a previous report, Seok et al. reported the effectiveness of mixing I and Br as $MAPbI_{3-x}Br_x$, showing 16.5% efficiency [72]. By increasing the ratio of Br, photovoltage is increased while the photo-absorption region becomes narrower. Inclusion of FA and Br is expected to increase photocurrent and photovoltage, respectively. Seok et al. obtained the best result (18.4%) by mixing $FAPbI_3$ and $MAPbBr_3$ in a 85:15 ratio. Following this report the compound $(FAPbI_3)_{0.85}(MAPbBr_3)_{0.15}$ become one of the standard perovskite materials. Zhao et al. (Nov. 12, 2014) prepared $HPbI_3$ as a precursor material for perovskite preparation [101]. By using $HPbI_3$, highly uniform formamidinium lead iodide ($FAPbI_3$) films were obtained through a one-step spin-coating process leading to 17.5% efficiency in a cell.

Until the end of 2014, eight papers reporting efficiencies higher than 16% on the basis of the modification of device preparation methods were submitted. Among them, 4 cases were planar heterojunction type cells: 17.91% [102], 17.3% [103], 16.97% [104], and 16.8% [105]. 2 cases were inverted type cells: 17.7% [106] and 17.1% [107]. One case (16.07% [108]) was a typical mesoscopic cell, featuring a hot-pressing method. The other one is a meso-superstructured cell: 16.7% [109]. Various methods were developed to obtain pure, well crystallized, and dense perovskite layers. However, there might be a limitation for these perovskites in terms of photo-absorption region and photovoltage. For drastic improvements, modification of perovskite composition would be necessary.

On Feb. 14, 2015, Seok et al. submitted a paper reporting 20.2% efficiency, together with certified data for 20.1% efficiency [110]. The key point was "intramolecular exchange". During the preparation of $FAPbI_3$ by the conventional two-step method, the PbI_2 layer with 290

nm thickness must be converted to a layer with 570 nm thickness to allow the insertion of FAI. To reduce such volume change, they prepared PbI_2-DMSO precursor, which was dissolved in DMF for the film preparation. Since the DMSO molecules are easily replaced with FAI, the PbI_2-DMSO layer with 510 nm thickness was converted to a $FAPbI_3$ layer with 560 nm thickness. Such methodology was applied to the mixed cation/mixed halogen compound, $(FAPbI_3)_{1-x}(MAPbBr_3)_x$. In this case, x was estimated to be 0.05, slightly different from the former case (x = 0.15 [100]). The features of the device are a thin (150 nm) mesoporous TiO_2 layer and a hole transport layer composed of PTAA. This paper was published on May 21, 2015, establishing the advantage of mixed cation/mixed halogen systems.

Utilization of DMSO adducts also improved the efficiency of $MAPbI_3$ devices. Park et al. (May 16, 2015) reported 19.7% efficiency by the use of $MAPbI_3$ prepared from MAI-PbI_2-DMSO in DMF followed by diethylether as an antisolvent [111]. The formation of precursor compound, $MA_2Pb_3I_8$-2DMSO was suggested by Yao et al. (May 2, 2015 [112]) and Nakamura et al. (Oct. 9, 2015 [113]) using crystallographic analysis. Another plausible intermediate structure was presented by Zheng et al. (Jul. 18, 2016) with 19.0% efficiency [114]. Nazeeruddin et al. (Aug. 18, 2015) found that PbI_2-rich precursor solution (PbI_2:MAI = 1.1:1) affords better performance up to 19.09% than the stoichiometric case [115]. On the other hand, Park et al. (Jan. 11, 2016) reported that excess MAI affords better performance up to 20.4% efficiency [116]. As seen here, the role of DMSO and the best material composition was still under investigation.

The mixed cation/mixed halogen compound, $(FAPbI_3)_{1-x}$ $(MAPbBr_3)_x$, resulted in superior performance for mesoscopic type devices. Nazeeruddin, Grätzel, and Hagfeldt et al. (Aug. 26, 2015) investigated the effect of PbI_2-rich material, by changing the PbI_2/FAI ratio, while fixing PbI_2/$PbBr_2$ ratio (0.85:0.15) and $PbBr_2$/MABr ratio (1:1) [117]. The highest efficiency (20.8%) was obtained for the PbI_2/FAI = 1.05:1 case. Seok et al. (Oct. 25, 2016) reported 20.1% efficiency by adding 5.7 mol% PbI_2 to $(FAPbI_3)_{0.85}(MAPbBr_3)_{0.15}$ [118]. The latter paper [118] was published on Dec. 3, 2015, earlier than the former one [117] on Jan. 1, 2016. Hagfeldt et al. (Jan. 5, 2016) further investigated the best ratio of MA, FA, I, and Br, and obtained 20.7% efficiency for $MA_{2/6}FA_{4/6}Pb(Br_{1/6}I_{5/6})_3$ sample [119]. Concerning the preparation method, Grätzel et al. (Dec. 5, 2015) reported chemical conversion of

a mesoporous lead halide layer to a compact perovskite layer [120]. The mesoporous lead halide (PbI_2/$PbBr_2$) layer was constructed by spin-coating their solutions in DMSO/DMF (2:8) mixed solvent. They achieved 20.75% efficiency. Hagfeldt et al. (Feb. 1, 2016) adjusted the concentration of the solution for spin-coating to modify the thickness of the perovskite layer, and achieved 20.8% efficiency [121]. Grätzel et al. (Apr. 2, 2016) reported a vacuum flash-assisted solution process, in which the sample was treated with vacuum after the spin-coating process [122]. They prepared 1.2×1.2 cm^2 devices using precursor solutions with $FA_{0.81}MA_{0.15}PbI_{2.51}Br_{0.45}$- DMSO composition, and obtained 20.5% efficiency with a 0.16 cm^2 mask, and 20.3% efficiency with a 1.00 cm^2 mask, respectively. They also obtained a certified 19.56% efficiency for an area of 1.00 cm^2. Modification of the TiO_2 layer and the hole-transport layer has been also resulted in high efficiency. Abate et al. (Sep. 17, 2015) reported Nd-doping of mesostructured TiO_2 with a result of 18.2% efficiency [123]. Concerning hole-transport materials for $FA_{1-x}MA_xPbI_{3-y}Br_y$, Cu(II) phthalocyanine-doped spiro-OMeTAD (19.35%, Jul. 2, 2015 [124]), bis(N,N-di-p-methoxyphenylamino)fluorene-dithiophene (20.2%, Sep. 7, 2015 [125]), branched methoxydiphenylamine-substituted fluorene derivatives (19.96%, Dec. 29, 2015 [126]), tetrakis(N,N-di-p-methoxyphenylamino)-spiro-[fluorene-9,9'-xanthene] (19.84%, Jan. 7, 2016 [127]), and bis(N,N-di-p-methoxyphenylamino)-spiro-[fluorene-9,9'-xanthene] (19.8%, Feb. 3, 2016 [128]) were reported.

On Dec. 24, 2015, Saliba et al. submitted a paper reporting triple cation perovskite solar cells, in which small amount of cesium was added to the mixed cation/mixed halogen perovskite [129]. They achieved 21.1% efficiency by adding 5% cesium ($Cs_{0.05}(MA_{0.17}FA_{0.83})_{0.95}Pb(I_{0.83}Br_{0.17})_3$). Correa-Baena et al. (Apr. 18, 2016) prepared triple cation perovskite solar cells with 19.7% efficiency and observed their degradation due to metal migration [130]. Grätzel et al. (May 4, 2016) added poly(methyl methacrylate) (PMMA) to the perovskite layer to achieve 21.6% efficiency [131]. They prepared the $[(FAI)_{0.81}(PbI_2)_{0.85}(MAPbBr_3)_{0.15}]$ precursor solution in a mixed solvent of N,N-dimethylformamide (DMF), N-methyl-2-pyrrolidone (NMP), and dimethylsulfoxide (DMSO), where the molar ratio of DMF/DMSO was 5:1, and the molar ratio of Pb^{2+}/$[(DMSO)_{0.8}(NMP)_{0.2}]$ was 1:1. They also prepared the PMMA solution in a mixed solvent of chlorobenzene and toluene (9:1 v/v). The perovskite precursor solution was spin-coated and

the PMMA solution was put in at the last moment of the spin-coating process. Gratzel et al. (Jul. 18, 2016) proposed the incorporation of Rb^+ into perovskites, and investigated RbFA, RbCsFA, RbMAFA, and RbCsMAFA systems [132]. The RbCsMAFA system achieved 21.8% efficiency by I-V measurement and 21.6% efficiency by MPPT measurement. The RbCsMAFA-based perovskite precursor was prepared by adding 1.5 M stock solution of RbI in DMF:DMSO 4:1 (v:v) to the CsMAFA precursor, which was prepared by adding 1.5 M stock solution of CsI in DMSO to the MAFA precursor, which was prepared by dissolving FAI (1 M), PbI_2 (1.1 M), MABr (0.2 M), and $PbBr_2$ (0.22 M) in DMF:DMSO 4:1 (v:v). The solution was prepared so that the cation ratio became the desired one. Therefore, the I:Br ratio may be varied slightly. The highest efficiency was obtained for a limited area of the device using a mask, resulting in a Voc of 1.18 V, while the fully illuminated device without mask produced a Voc of 1.24 V. This paper was published online on Sep. 29, 2016.

Concerning planar hetero-junction perovskite solar cells, efficiencies higher than 18% was reported in only one case [73] before July 2015. Park et al. (Jul. 2, 2015) reported a planar hetero-junction cell using mixed cation perovskites, $FA_{1-x}Cs_xPbI_3$ [133]. The device using $FA_{0.9}Cs_{0.1}PbI_3$ exhibited 13.9% efficiency for forward scan, and 19.0% efficiency for reverse scan. Hagfeldt et al. (Aug. 24, 2015) applied the mixed cation/mixed halogen perovskite, $(FAPbI_3)_{0.85}(MAPbBr_3)_{0.15}$, to planar hetero-junction cells [134]. In this case, a TiO_2 compact layer did not work well, while a SnO_2-based device achieved 18.4% efficiency. Ito et al. (Aug. 25, 2015) achieved 19.4% efficiency [135] by the modification of "fast deposition-crystallization" [74], using concentrated precursor solution. Segawa et al. (Oct. 7, 2015) investigated the origin of I-V hysteresis, using a device with 18.0% efficiency [136]. D. S. Kim et al. (Nov. 27, 2015) prepared planar hetero-junction cells based on mixed cation/mixed halogen perovskites, which were prepared by the reaction of PbI_2, PbI_2-DMSO complex, or PbI_2-NMP complex with $(FAI)_{0.75}(MABr)_{0.15}$ [137]. The device based on the perovskite derived from the PbI_2-NMP complex showed 19.5% efficiency. Im et al. (Nov. 29, 2015) prepared pure $MAPbI_{3-x}Cl_x$ powder by the reaction of 3:1 MAI and $PbCl_2$ in iso-propanol, followed by repeated centrifugation and washing [138]. By dissolving the pure powder of $MAPbI_{3-x}Cl_x$ in DMF with HI as an additive, slow speed spin-coating afforded thick perovskite layers up to 900 nm. The device with a thin PTAA hole transporting layer

exhibited 19.1% efficiency. Y. Yan et al. (Jan. 31, 2016) added 5% $Pb(SCN)_2$ to the precursor solution of $MAPbI_3$ [139]. Although the SCN^- ion was not included in the final perovskite layer, the improved crystalline quality achieved 19.45% efficiency for a planar hetero-junction device using a SnO_2 compact layer covered with PCBM. Abate et al. (Apr. 11, 2016) added 5 mol% methylammonium formate to the precursor solution to achieve 19.5% efficiency for a planar hetero-junction device using a SnO_2 compact layer [140]. M. J. Ko et al. (Jun. 20, 2016) prepared Nb-doped TiO_2 compact layers with an UV-assisted solution process under 50°C, and then formed perovskite layers by spin-coating a DMF solution of MAI, PbI_2, and DMSO, followed by diethylether dripping [141]. The planar hetero-junction device achieved 19.57% efficiency. S. Liu et al. (Jul. 25, 2016) modified the surface of a TiO_2 compact layer with an ionic liquid, 1-butyl-3-methylimidazolium tetrafluoroborate, to achieve 19.62% efficiency for a $MAPbI_3$ device [142]. Correa-Baena et al. (Aug. 16, 2016) prepared SnO_2 compact layers with a combination of spin-coating of a $SnCl_4$ precursor solution and post-treatment by chemical bath depositon, and then formed triple cation (MA, FA, Cs)/ mixed halogen (I, Br) perovskite layers, to achieve 20.8% efficiency in a planar hetero-junction device [143]. Finally, a planar device reached 20% efficiency. This paper was published online on Sep. 15, 2016. In the case of inverted structure devices, efficiencies higher than 18% were reported in several papers [144-148]. Huang et al. (Feb. 18, 2016) reported 20.3% efficiency from the use of a thin polystylene layer between the perovskite and C_{60} layers [149]. As a certified efficiency under standard conditions (area larger than 1 cm^2), L. Han et al. (May 28, 2016) reported 18.21% for an inverted structure device [150]. Optimization of inverted structure devices is also advancing rapidly.

CONCLUSION

Most of the recent highly efficient perovskite solar cells are characterized by two keywords, "solvent engineering" and "compositional engineering". By the development of anti-solvent method, most of perovskite layers were formed using one-step spin-coating. Successful preparation of perovskite $(FAPbI_3)_{0.85}(MAPbBr_3)_{0.15}$ was a big breakthrough. Although the details of the device showing the highest efficiency (22.1%) have not yet been disclosed, it would be an extension of the present approaches. One planar device and one inverted structure device were reported with efficiencies higher than 20%,

but most of the devices showing efficiencies higher than 20% are based on mesoscopic structure. Investigations of the reason why mesoscopic structure affords better performances may bring further improvements in perovskite solar cells.

References

[1] M. A. Green, K. Emery, Y. Hishikawa, W. Warta, E. D. Dunlop, D. H. Levi, A. W. Y. Ho-Baillie, Prog. Photovolt. Res. Appl. 25 (2017) 3-13.

[2] https://www.nrel.gov/pv/assets/images/efficiency-chart.png

[3] A. Hagfeldt, G. Boschloo, L. Sun, L. Kloo, H. Pettersson, Chem. Rev. 110 (2010) 6595-6663.

[4] P. V. Kamat, Acc. Chem. Res. 45 (2012) 1906-1915.

[5] A. Kojima, K. Teshima, Y. Shirai, T. Miyasaka, J. Am. Chem. Soc. 131 (2009) 6050-6051.

[6] T. Miyasaka, J. Phys. Chem. Lett. 2 (2011) 262-269.

[7] J.-H. Im, C.-R. Lee, J.-W. Lee, S.-W. Park, N.-G. Park, Nanoscale 3 (2011) 4088-4093.

[8] J.-H. Im, J. Chung, S.-J. Kim, N.-G. Park, Nanoscale Res. Lett. 7 (2012) 353.

[9] A. Kojima, M. Ikegami, K. Teshima, T. Miyasaka, Chem. Lett. 41 (2012) 397-399.

[10] M. M. Lee, J. Teuscher, T. Miyasaka, T. N. Murakami, H. J. Snaith, Science 338 (2012) 643-647.

[11] H.-S. Kim, C.-R. Lee, J.-H. Im, K.-B. Lee, T. Moehl, A. Marchioro, S.-J. Moon, R. Humphry-Baker, J.-H. Yum, J. E. Moser, M. Grätzel, N.-G. Park, Scientific Reports 2 (2012) 591.

[12] J. H. Heo, S. H. Im, J. H. Noh, T. N. Mandal, C.-S. Lim, J. A. Chang, Y. H. Lee, H.-J. Kim, A. Sarkar, M. K. Nazeeruddin, M. Grätzel, S. I. Seok, Nature Photonics 7 (2013) 486-491.

[13] A. Yella, H.-W. Lee, H. N. Tsao, C. Yi, A. K. Chandiran, M. K. Nazeerddin, E. W.-G. Diau, C.-Y. Yeh, S. M. Zakeeruddin, M. Grätzel, Science 334 (2011) 629-634.

[14] L. Etgar, P. Gao, Z. Xue, Q. Peng, A. K. Chandiran, B. Liu, M. K. Nazeeruddin, M. Grätzel, J. Am. Chem. Soc. 134 (2012) 17396-17399.

[15] E. J. W. Crossland, N. Noel, V. Sivaram, T. Leijtens, J. A. Alexander-Webber, H. J. Snaith, Nature 495 (2013) 215-219.

[16] J. Qiu, Y. Qiu, K. Yan, M. Zhong, C. Mu, H. Yan, S. Yang, Nanoscale 5 (2013) 3245-3248.

[17] H.-S. Kim, J.-W. Lee, N. Yantara, P. P. Boix, S. A. Kulkarni, S. Mhaisalkar, M. Grätzel, N.-G. Park, Nano Lett. 13 (2013) 2412-2417.

[18] J. H. Noh, S. H. Im, J. H. Heo, T. N. Mandal, S. I. Seok, Nano Lett. 13 (2013) 1764-1769.

[19] B. Cai, Y. Xing, Z. Yang, W.-H. Zhang, J. Qiu, Energy Environ. Sci. 6 (2013) 1480-1485.

[20] E. Edri, S. Kirmayer, D. Cahen, G. Hodes, J. Phys. Chem. Lett. 4 (2013) 897-902.

[21] J. M. Ball, M. M. Lee, A. Hey, H. J. Snaith, Energy Environ. Sci. 6 (2013) 1739-1743.

[22] A. Abrusci, S. D. Stranks, P. Docampo, H.-L. Yip, A. K.-Y. Jen, H. J. Snaith, Nano Lett. 13 (2013) 3124-3128.

[23] D. Bi, L. Yang, G. Boschloo, A. Hagfeldt, E. M. J. Johansson, J. Phys. Chem. Lett. 4 (2013) 1532-1536.

[24] J.-Y. Jeng, Y.-F. Chiang, M.-H. Lee, S.-R. Peng, T.-F. Guo, P. Chen, T.-C. Wen, Adv. Mater. 25 (2013) 3727-3732.

[25] D. Bi, G. Boschloo, S. Schwarzmüller, L. Yang, E. M. J. Johansson, A. Hagfeldt, Nanoscale 5 (2013) 11686-11691.

[26] J. Burschka, N. Pellet, S.-J. Moon, R. Humphry-Baker, P. Gao, M. K. Nazeeruddin, M. Grätzel, Nature 499 (2013) 316-319.

[27] K. Liang, D. B. Mitzi, M. T. Prikas, Chem. Mater. 10 (1998) 403-411.

[28] T. Baikie, Y. Fang, J. M. Kadro, M. Schreyer, F. Wei, S. G. Mhaisalkar, M. Graetzel, T. J. White, J. Mater. Chem. A 1 (2013) 5628-5641.

[29] A. Poglitsch, D. Weber, J. Chem. Phys. 87 (1987) 6373.

[30] M. J. Carnie, C. Charbonneau, M. L. Davies, J. Troughton, T. M. Watson, K. Wojciechowski, H. Snaith, D. A. Worsley, Chem. Commun. 49 (2013) 7893-7895.

[31] W. Li, J. Li, L. Wang, G. Niu, R. Gao, Y. Qiu, J. Mater. Chem. A 1 (2013) 11735-11740.

[32] M. Liu, M. B. Johnston, H. J. Snaith, Nature 501 (2013) 395-398.

[33] G. E. Eperon, V. M. Burlakov, P. Docampo, A. Goriely, H. J. Snaith, Adv. Funct. Mater. 24 (2014) 151-157.

[34] M. Era, T. Hattori, T. Taira, T. Tsutsui, Chem. Mater. 9 (1997) 8-10.

[35] D. Bi, S.-J. Moon, L. Häggman, G. Boschloo, L. Yang, E. M. J. Johansson, M. K. Nazeeruddin, M. Grätzel, A. Hagfeldt, RSC Adv. 3 (2013) 18762-18766.

[36] W. Zhang, M. Saliba, S. D. Stranks, Y. Sun, X. Shi, U. Wiesner, H. J. Snaith, Nano Lett. 13 (2013) 4505-4510.

[37] T. Leijtens, G. E. Eperon, S. Pathak, A. Abate, M. M. Lee, H. J. Snaith, Nature Commun. 4 (2013) 2885.

[38] W. A. Laban, L. Etgar, Energy Environ. Sci. 6 (2013) 3249-3253.

[39] Y. Zhao, K. Zhu, J. Phys. Chem. Lett. 4 (2013) 2880-2884.

[40] S. Y. Dou, L. T. Yan, Y. C. Liu, G. Du, P. Zhou, J. Mater. Sci. Mater. Electron. 24 (2013) 4862-4867.

[41] K. Kakiage, T. Kyomen, M. Hanaya, Chem. Lett. 42 (2013) 1520-1521.

[42] F. Matteocci, S. Razza, F. Di Giacomo, S. Casaluci, G. Mincuzzi, T. M. Brown, A. D'Epifanio, S. Licoccia, A. Di Carlo, Phys. Chem. Chem. Phys. 16 (2014) 3918-3923.

[43] Y. Rong, Z. Ku, M. Xu, G. Liu, H. Wang, H. Han, Proc. SPIE 8830 (2013) 88301W.

[44] Z. Ku, Y. Rong, M. Xu, T. Liu, H. Han, Scientific Reports 3 (2013) 3132.

[45] M. H. Kumar, N. Yantara, S. Dharani, M. Graetzel, S. Mhaisalkar, P. P. Boix, N. Mathews, Chem. Commun. 49 (2013) 11089-11091.

[46] G. Niu, W. Li, F. Meng, L. Wang, H. Dong, Y. Qiu, J. Mater. Chem. A 2 (2014) 705-710.

[47] F. Di Giacomo, S. Razza, F. Matteocci, A. D'Epifanio, S. Licoccia, T. M. Brown, A. Di Carlo, J. Power Sources 251 (2014) 152.

[48] S. Dharani, H. K. Mulmudi, N. Yantara, P. T. T. Trang, N. G. Park, M. Graetzel, S. Mhaisalkar, N. Mathews, P. P. Boix, Nanoscale 6 (2014) 1675-1679.

[49] O. Malinkiewicz, A. Yella, Y. H. Lee, G. M. Espallargas, M. Graetzel, M. K. Nazeeruddin, H. J. Bolink, Nature Photonics 8 (2014) 128-132.

[50] D. Liu, T. L. Kelly, Nature Photonics 8 (2014) 133-138.

[51] H.-S. Kim, I. Mora-Sero, V. Gonzalez-Pedro, F. Fabregat-Santiago, E. J. Juarez-Perez, N.-G. Park, J. Bisquert, Nature Commun. 4 (2013) 2242.

[52] G. Xing, N. Mathews, S. Sun, S. S. Lim, Y. M. Lam, M. Grätzel, S. Mhaisalkar, T. C. Sum, Science 342 (2013) 344-347.

[53] S. D. Stranks, G. E. Eperon, G. Grancini, C. Menelaou, M. J. P. Alcocer, T. Leijtens, L. M. Herz, A. Petrozza, H. J. Snaith, Science 342 (2013) 341-344.

[54] A. Marchioro, J. Teuscher, D. Friedrich, M. Kunst, R. van de Krol, T. Moehl, M. Grätzel, J.-E. Moser, Nature Photonics 8 (2014) 250-255.

[55] A. Dualeh, T. Moehl, N. Tétreault, J. Teuscher, P. Gao, M. K. Nazeeruddin, M. Grätzel, ACS Nano 8 (2014) 362-373.

[56] A. Marchioro, J. C. Brauer, J. Teuscher, M. Grätzel, J.-E. Moser, Proc. SPIE 8811 (2013) 881108.

[57] S. Colella, E. Mosconi, P. Fedeli, A. Listorti, F. Gazza, F. Orlandi, P. Ferro, T. Besagni, A. Rizzo, G. Calestani, G. Gigli, F. De Angelis, R. Mosca, Chem. Mater. 25 (2013) 4613-4618.

[58] E. Mosconi, A. Amat, M. K. Nazeeruddin, M. Grätzel, F. De Angelis, J. Phys. Chem. C 117 (2013) 13902-13913.

[59] J. Even, L. Pedesseau, J.-M. Jancu, C. Katan, J. Phys. Chem. Lett. 4 (2013) 2999-3005.

[60] F. Brivio, A. B. Walker, A. Walsh, APL Mater. 1 (2013) 042111.

[61] A. Filippetti, A. Mattoni, Phys. Rev. B 89 (2014) 125203.

[62] L. Pedesseau, J.-M. Jancu, A. Rolland, E. Deleporte, C. Katan, J. Even, Opt. Quant. Electronics 10 (2014) 1225-1232.

[63] J. Bisquert, J. Phys. Chem. Lett. 4 (2013) 2597-2598.

[64] M. D. McGehee, Nature 501 (2013) 323-325.

[65] N.-G. Park, J. Phys. Chem. Lett. 4 (2013) 2423-2429.

[66] J. H. Rhee, C.-C. Chung, E. W.-G. Diau, NPG Asia Mater. 5 (2013) e68.

[67] H. S. Kim, S. H. Im, N.-G. Park, J. Phys. Chem. C 118 (2014) 5615-5625.

[68] H. J. Snaith, J. Phys. Chem. Lett. 4 (2013) 3623-3630.

[69] Q. Chen, H. Zhou, Z. Hong, S. Luo, H.-S. Duan, H.-H. Wang, Y. Liu, G. Li, Y. Yang, J. Am. Chem. Soc. 136 (2014) 622-625.

[70] K. Wojciechowski, M. Saliba, T. Leijtens, A. Abate, H. J. Snaith, Energy Environ. Sci. 7 (2014) 1142-1147.

[71] J.-H. Im, I.-H. Jang, N. Pellet, M. Grätzel, N.-G. Park, Nature Nanotechnology 9 (2014) 927-932.

[72] N. J. Jeon, J. H. Noh, Y. C. Kim, W. S. Yang, S. Ryu, S. I. Seok, Nature Mater. 13 (2014) 897-903.

[73] H. Zhou, Q. Chen, G. Li, S. Luo, T.-b. Song, H.-S. Duan, Z. Hong, J. You, Y. Liu, Y. Yang, Science 345 (2014) 542-546.

[74] M. Xiao, F. Huang, W. Huang, Y. Dkhissi, Y. Zhu, J. Etheridge, A. Gray-Weale, U. Bach, Y.-B. Cheng, L. Spiccia, Angew. Chem. Int. Ed. 53 (2014) 9898-9903.

[75] F. Hao, C. C. Stoumpos, D. H. Cao, R. P. H. Chang, M. G. Kanatzidis, Nature Photonics 8 (2014) 489-494.

[76] Y. Ogomi, A. Morita, S. Tsukamoto, T. Saitho, N. Fujikawa, Q. Shen, T. Toyoda, K. Yoshino, S. S. Pandey, T. Ma, S. Hayase, J. Phys. Chem. Lett. 5 (2014) 1004-1011.

[77] I. Chung, B. Lee, J. He, R. P. H. Chang, M. G. Kanatzidis, Nature 485 (2012) 486-489.

[78] F. Hao, C. C. Stoumpos, R. P. H. Chang, M. G. Kanatzidis, J. Am. Chem. Soc. 136 (2014) 8094-8099.

[79] N. K. Noel, S. D. Stranks, A. Abate, C. Wehrenfennig, S. Guarnera, A. A. Haghighirad, A. Sadhanala, G. E. Eperon, S. K. Pathak, M. B. Johnston, A. Petrozza, L. M. Herz, H. J. Snaith, Energy Environ. Sci. 7 (2014) 3061-3068.

[80] M. H. Kumar, S. Dharani, W. L. Leong, P. P. Boix, R. R. Prabhakar, T. Baikie, C. Shi, H. Ding, R. Ramesh, M. Asta, M. Graetzel, S. G. Mhaisalkar, N. Mathews, Adv. Mater. 26 (2014) 7122-7127.

[81] E. Edri, S. Kirmayer, M. Kulbak, G. Hodes, D. Cahen, J. Phys. Chem. Lett. 5 (2014) 429-433.

[82] S. A. Kulkarni, T. Baikie, P. P. Boix, N. Yantara, N. Mathews, S. Mhaisalkar, J. Mater. Chem. A 2 (2014) 9221-9225.

[83] Y. Zhao, K. Zhu, J. Am. Chem. Soc. 136 (2014) 12241-12244.

[84] N. Pellet, P. Gao, G. Gregori, T.-Y. Yang, M. K. Nazeeruddin, J. Maier, M. Grätzel, Angew. Chem. Int. Ed. 53 (2014) 3151-3157.

[85] T. M. Koh, K. Fu, Y. Fang, S. Chen, T. C. Sum, N. Mathews, S. G. Mhaisalkar, P. P. Boix, T. Baikie, J. Phys. Chem. C 118 (2014) 16458-16462.

[86] G. E. Eperon, S. D. Stranks, C. Menelaou, M. B. Johnston, L. M. Herz, H. J. Snaith, Energy Environ. Sci. 7 (2014) 982-988.

[87] S. Pang, H. Hu, J. Zhang, S. Lv, Y. Yu, F. Wei, T. Qin, H. Xu, Z. Liu, G. Cui, Chem. Mater. 26 (2014) 1485-1491.

[88] J.-W. Lee, D.-J. Seol, A.-N. Cho, N.-G. Park, Adv. Mater. 26 (2014) 4991-4998.

[89] S. Lv, S. Pang, Y. Zhou, N. P. Padture, H. Hu, L. Wang, X. Zhou, H. Zhu, L. Zhang, C. Huang, G. Cui, Phys. Chem. Chem. Phys. 16 (2014) 19206-19211.

[90] F. C. Hanusch, E. Wiesenmayer, E. Mankel, A. Binek, P. Angloher, C. Fraunhofer, N. Giesbrecht, J. M. Feckl, W. Jaegermann, D. Johrendt, T. Bein, P. Docampo, J. Phys. Chem. Lett. 5 (2014) 2791-2795.

[91] N. K. Noel, A. Abate, S. D. Stranks, E. S. Parrott, V. M. Burlakov, A. Goriely, H. J. Snaith, ACS Nano 8 (2014) 9815-9821.

[92] C.-H. Chiang, Z.-L. Tseng, C.-G. Wu, J. Mater. Chem. A 2 (2014) 15897-15903.

[93] Q. Lin, A. Armin, R. C. R. Nagiri, P. L. Burn, P. Meredith, Nature Photonics 9 (2015) 106-112.

[94] N. J. Jeon, H. G. Lee, Y. C. Kim, J. Seo, J. H. Noh, J. Lee, S. I. Seok, J. Am. Chem. Soc. 136 (2014) 7837-7840.

[95] S. Ryu, J. H. Noh, N. J. Jeon, Y. C. Kim, W. S. Yang, J. W. Seo, S. I. Seok, Energy Environ. Sci. 7 (2014) 2614-2618.

[96] J. Luo, J.-H. Im, M. T. Mayer, M. Schreier, M. K. Nazeeruddin, N.-G. Park, S. D. Tilley, H. J. Fan, M. Grätzel, Science 345 (2014) 1593-1596.

[97] J. T.-W. Wang, J. M. Ball, E. M. Barea, A. Abate, J. A. Alexander-Webber, J. Huang, M. Saliba, I. Mora-Sero, J. Bisquert, H. J. Snaith, R. J. Nicholas, Nano Lett. 14 (2014) 724-730.

[98] A. Abate, M. Saliba, D. J. Hollman, S. D. Stranks, K. Wojciechowski, R. Avolio, G. Grancini, A. Petrozza, H. J. Snaith, Nano Lett. 14 (2014) 3247-3254.

[99] H. J. Snaith, A. Abate, J. M. Ball, G. E. Eperon, T. Leijtens, N. K. Noel, S. D. Stranks, J. T.-W. Wang, K. Wojciechowski, W. Zhang, J. Phys. Chem. Lett. 5 (2014) 1511-1515.

[100] N. J. Jeon, J. H. Noh, W. S. Yang, Y. C. Kim, S. Ryu, J. Seo, S. I. Seok, Nature 517 (2015) 476-480.

[101] F. Wang, H. Yu, H. Xu, N. Zhao, Adv. Funct. Mater. 25 (2015) 1120-1126.

[102] Q. Chen, H. Zhou, Y. Fang, A. Z. Stieg, T.-B. Song, H.-H. Wang, X. Xu, Y. Liu, S. Lu, J. You, P. Sun, J. McKay, M. S. Goorsky, Y. Yang, Nature Commun. 6 (2015) 7269.

[103] K. Wojciechowski, S. D. Stranks, A. Abate, G. Sadoughi, A. Sadhanala, N. Kopidakis, G. Rumbles, C.-Z. Li, R. H. Friend, A. K.-Y. Jen, H. J. Snaith, ACS Nano 8 (2014) 12701-12709.

[104] F. Huang, Y. Dkhissi, W. Huang, M. Xiao, I. Benesperi, S. Rubanov, Y. Zhu, X. Lin, L. Jiang, Y. Zhou, A. Gray-Weale, J. Etheridge, C. R. McNeill, R. A. Caruso, U. Bach, L. Spiccia, Y.-B. Cheng, Nano Energy 10 (2014) 10-18.

[105] Y. Li, J. K. Cooper, R. Buonsanti, C. Giannini, Y. Liu, F. M. Toma, I. D. Sharp, J. Phys. Chem. Lett. 6 (2015) 493-499.

[106] W. Nie, H. Tsai, R. Asadpour, J.-C. Blancon, A. J. Neukirch, G. Gupta, J. J. Crochet, M. Chhowalla, S. Tretiak, M. A. Alam, H.-L. Wang, A. D. Mohite, Science 347 (2015) 522-525.

[107] J. You, Y. M. Yang, Z. Hong, T.-B. Song, L. Meng, Y. Liu, C. Jiang, H. Zhou, W.-H. Chang, G. Li, Y. Yang, Appl. Phys. Lett. 105 (2014) 183902.

[108] M. Lv, X. Dong, X. Fang, B. Lin, S. Zhang, J. Ding, N. Yuan, RSC Adv. 5 (2015) 20521-20529.

[109] S. Pathak, A. Sepe, A. Sadhanala, F. Deschler, A. Haghighirad, N. Sakai, K. C. Goedel, S. D. Stranks, N. Noel, M. Price, S. Hüttner, N. A. Hawkins, R. H. Friend, U. Steiner, H. J. Snaith, ACS Nano 9 (2015) 2311-2320.

[110] W. S. Yang, J. H. Noh, N. J. Jeon, Y. C. Kim, S. Ryu, J. Seo, S. I. Seok, Science 348 (2015) 1234-1237.

[111] N. Ahn, D.-Y. Son, I.-H. Jang, S. M. Kang, M. Choi, N.-G. Park, J. Am. Chem. Soc. 137 (2015) 8696-8699.

[112] Y. Rong, Z. Tang, Y. Zhao, X. Zhong, S. Venkatesan, H. Graham, M. Patton, Y. Jing, A. M. Guloy, Y. Yao, Nanoscale 7 (2015) 10595-10599.

[113] Y. Guo, K. Shoyama, W. Sato, Y. Matsuo, K. Inoue, K. Harano, C. Liu, H. Tanaka, E. Nakamura, J. Am. Chem. Soc. 137 (2015) 15907-15914.

[114] J. Cao, X. Jing, J. Yan, C. Hu, R. Chen, J. Yin, J. Li, N. Zheng, J. Am. Chem. Soc. 138 (2016) 9919-9926.

[115] C. Roldán-Carmona, P. Gratia, I. Zimmermann, G. Grancini, P. Gao, M. Graetzel, M. K. Nazeeruddin, Energy Environ. Sci. 8 (2015) 3550-3556.

[116] D.-Y. Son, J.-W. Lee, Y. J. Choi, I.-H. Jang, S. Lee, P. J. Yoo, H. Shin, N. Ahn, M. Choi, D. Kim, N.-G. Park, Nature Energy 1 (2016) 16081.

[117] D. Bi, W. Tress, M. I. Dar, P. Gao, J. Luo, C. Renevier, K. Schenk, A. Abate, F. Giordano, J.-P. Correa Baena, J.-D. Decoppet, S. M. Zakeeruddin, M. K. Nazeeruddin, M. Grätzel, A. Hagfeldt, Sci. Adv. 2 (2016) e1501170.

[118] Y. C. Kim, N. J. Jeon, J. H. Noh, W. S. Yang, J. Seo, J. S. Yun, A. Ho-Baillie, S. Huang, M. A. Green, J. Seidel, T. K. Ahn, S. I. Seok, Adv. Energy Mater. 6 (2016) 1502104.

[119] T. J. Jacobsson, J.-P. Correa-Baena, M. Pazoki, M. Saliba, K. Schenk, M. Grätzel, A. Hagfeldt, Energy Environ. Sci. 9 (2016) 1706-1724.

[120] C. Yi, X. Li, J. Luo, S. M. Zakeeruddin, M. Grätzel, Adv. Mater. 28 (2016) 2964-2970.

[121] J.-P. Correa-Baena, M. Anaya, G. Lozano, W. Tress, K. Domanski, M. Saliba, T. Matsui, T. J. Jacobsson, M. E. Calvo, A. Abate, M. Grätzel, H. Míguez, A. Hagfeldt, Adv. Mater. 28 (2016) 5031-5037.

[122] X. Li, D. Bi, C. Yi, J.-D. Décoppet, J. Luo, S. M. Zakeeruddin, A. Hagfeldt, M. Grätzel, Science 353 (2016) 58-62.

[123] B. Roose, K. C. Gödel, S. Pathak, A. Sadhanala, J. P. C. Baena, B. D. Wilts, H. J. Snaith, U. Wiesner, M. Grätzel, U. Steiner, A. Abate, Adv. Energy Mater. 6 (2016) 1501868.

[124] J. Seo, N. J. Jeon, W. S. Yang, H.-W. Shin, T. K. Ahn, J. Lee, J. H. Noh, S. I. Seok, Adv. Energy Mater. 2015 (2015) 1501320.

[125] M. Saliba, S. Orlandi, T. Matsui, S. Aghazada, M. Cavazzini, J.-P. Correa-Baena, P. Gao, R. Scopelliti, E. Mosconi, K.-H. Dahmen, F. De Angelis, A. Abate, A. Hagfeldt, G. Pozzi, M. Graetzel, M. K. Nazeeruddin, Nature Energy 1 (2016) 15017.

[126] T. Malinauskas, M. Saliba, T. Matsui, M. Daskeviciene, S. Urnikaite, P. Gratia, R. Send, H. Wonneberger, I. Bruder, M. Graetzel, V. Getautis, M. K. Nazeeruddin, Energy Environ. Sci. 9 (2016) 1681-1686.

[127] B. Xu, D. Bi, Y. Hua, P. Liu, M. Cheng, M. Grätzel, L. Kloo, A. Hagfeldt, L. Sun, Energy Environ. Sci. 9 (2016) 873-877.

[128] D. Bi, B. Xu, P. Gao, L. Sun, M. Grätzel, A. Hagfeldt, Nano Energy 23 (2016) 138-144.

[129] M. Saliba, T. Matsui, J.-Y. Seo, K. Domanski, J.-P. Correa-Baene, M. K. Nazeeruddin, S. M. Zakeeruddin, W. Tress, A. Abate, A. Hagfeldt, M. Grätzel, Energy Environ. Sci. 9 (2016) 1989-1997.

[130] K. Domanski, J.-P. Correa-Baena, N. Mine, M. K. Nazeeruddin, A. Abate, M. Saliba, W. Tress, A. Hagfeldt, M. Grätzel, ACS Nano 10 (2016) 6306-6314.

[131] D. Bi, C. Yi, J. Luo, J.-D. Décoppet, F. Zhang, S. M. Zakeeruddin, X. Li, A. Hagfeldt, M. Grätzel, Nature Energy 1 (2016) 16142.

[132] M. Saliba, T. Matsui, K. Domanski, J.-Y. Seo, A. Ummadisingu, S. M. Zakeeruddin, J.-P. Correa-Baena, W. R. Tress, A. Abate, A. Hagfeldt, M. Gratzel, Science 354 (2016) 206-209.

[133] J.-W. Lee, D.-H. Kim, H.-S. Kim, S.-W. Seo, S. M. Cho, N.-G. Park, Adv. Energy Mater. 2015 (2015) 1501310.

[134] J. P. Correa Baena, L. Steier, W. Tress, M. Saliba, S. Neutzner, T. Matsui, F.

Giordano, T. J. Jacobsson, A. R. S. Kandada, S. M. Zakeeruddin, A. Petrozza, A. Abate, M. K. Nazeeruddin, M. Grätzel, A. Hagfeldt, Energy Environ. Sci. 8 (2015) 2928-2934.

[135] H. D. Kim, H. Ohkita, H. Benten, S. Ito, Adv. Mater. 28 (2016) 917-922.

[136] L. Cojocaru, S. Uchida, P. V. V. Jayaweera, S. Kaneko, J. Nakazaki, T. Kubo, H. Segawa, Chem. Lett. 44 (2015) 1750-1752.

[137] Y. Jo, K. S. Oh, M. Kim, K.-H. Kim, H. Lee, C.-W. Lee, D. S. Kim, Adv. Mater. Interfaces 3 (2016) 1500768.

[138] J. H. Heo, S. H. Im, Nanoscale, 2016, 8, 2554-2560.

[139] W. Ke, C. Xiao, C. Wang, B. Saparov, H.-S. Duan, D. Zhao, Z. Xiao, P. Schulz, S. P. Harvey, W. Liao, W. Meng, Y. Yu, A. J. Cimaroli, C.-S. Jiang, K. Zhu, M. Al-Jassim, G. Fang, D. B. Mitzi, Y. Yan, Adv. Mater. 28 (2016) 5214-5221.

[140] J.-Y. Seo, T. Matsui, J. Luo, J.-P. Correa-Baena, F. Giordano, M. Saliba, K. Schenk, A. Ummadisingu, K. Domanski, M. Hadadian, A. Hagfeldt, S. M. Zakeeruddin, U. Steiner, M. Grätzel, A. Abate, Adv. Energy Mater. 6 (2016) 1600767.

[141] I. Jeong, H. Jung, M. Park, J. S. Park, H. J. Son, J. Joo, J. Lee, M. J. Ko, Nano Energy 28 (2016) 380-389.

[142] D. Yang, X. Zhou, R. Yang, Z. Yang, W. Yu, X. Wang, C. Li, S. Liu, R. P. H. Chang, Energy Environ. Sci. 9 (2016) 3071-3078.

[143] E. H. Anaraki, A. Kermanpur, L. Steier, K. Domanski, T. Matsui, W. Tress, M. Saliba, A. Abate, M. Gratzel, A. Hagfeldt, J.-P. Correa-Baena, Energy Environ. Sci. 9 (2016) 3128-3134.

[144] J. H. Heo, H. J. Han, D. Kim, T. K. Ahn, S. H. Im, Energy Environ. Sci. 8 (2015) 1602-1608.

[145] C. Bi, Q. Wang, Y. Shao, Y. Yuan, Z. Xiao, J. Huang, Nature Commun. 6 (2015) 7747.

[146] C.-G. Wu, C,-H, Chiang, Z.-L. Tseng, M. K. Nazeeruddin, A. Hagfeldt, M. Grätzel, Energy Environ. Sci. 8 (2015) 2725-2733.

[147] Q. Dong, Y. Yuan, Y. Shao, Y. Fang, Q. Wang, J. Huang, Energy Environ. Sci. 8 (2015) 2464-2470.

[148] H. Sung, N. Ahn, M. S. Jang, J.-K. Lee, H. Yoon, N.-G. Park, M. Choi, Adv. Energy Mater. 6 (2016) 1501873.

[149] Q. Wang, Q. Dong, T. Li, A. Gruverman, J. Huang, Adv. Mater. 28 (2016) 6734-6739.

[150] Y. Wu, X. Yang, W. Chen, Y. Yue, M. Cai, F. Xie, E. Bi, A. Islam, L. Han, Nature Energy 1 (2016) 16148.

Jotaro Nakazaki is an an assistant professor in the Research Center for Advanced Science and Technology (RCAST), The University of Tokyo. He took his PhD (2000) at the Department of Basic Science, Graduate School of Arts and Sciences, The University of Tokyo. He was a post-doc in the same department (2000-2001), Gakushuin University (2001-2002), and the Department of General Systems Studies, Graduate School of Arts and Sciences, The University of Tokyo (2002-2006). Since 2006, he has been working on the development of organic photovoltaics at RCAST.

Hiroshi Segawa is a professor of the University of Tokyo. He was awarded the degree of Doctor of Engineering by Kyoto University in 1989. He was a research associate (1989-1995) at the division of Molecular Engineering, Graduate School of Engineering, Kyoto University. In 1995 he joined the University of Tokyo as Associate Professor. From 1997 he has also been in charge of the Department of Applied Chemistry at the Graduate School of Engineering. From 2006 he joined RCAST as a professor. In 2010, he was appointed director of the Academic-Industrial Joint Laboratory for Renewable Energy of RCAST. From 2016 he has also been in charge of the Department of General Systems Studies, Graduate School of Arts and Sciences, The University of Tokyo.